

Synthesis, enantiomeric separation and docking studies of spiropiperidine analogues as ligands of the nociceptin/orphanin FQ receptor†

Cite this: DOI: 10.1039/c4md00082j

Umberto M. Battisti,^a Sandra Corrado,^a Claudia Sorbi,^a Andrea Cornia,^b Annalisa Tait,^a Davide Malfacini,^c Maria Camilla Cerlesi,^c Girolamo Calò^c and Livio Brasili^{*a}

Received 24th February 2014

Accepted 22nd April 2014

DOI: 10.1039/c4md00082j

www.rsc.org/medchemcomm

A series of triazospirodecanone derivatives were synthesized as potential NOP ligands. 8-(Chroman-4-yl)-1-phenyl-1,3,8-triazaspiro[4.5]decan-4-one (**4**) and its 5-fluoro analogue (**18**) proved to be active as agonists with EC₅₀ values in the submicromolar range. Single enantiomers of compound **4** were separated and tested as NOP agonists; the eutomer *R*-(+)-**4** showed a pEC₅₀ of 7.34. Finally docking studies were performed on the NOP receptor to identify the most significant stereospecific interactions.

Introduction

Since their discovery, many advances have been made regarding the biological significance and functions of the neuropeptide nociceptin/orphanin FQ (N/OFQ) and its receptor, namely the N/OFQ peptide (NOP) receptor.^{1–6} Indeed several studies suggested that the N/OFQ–NOP receptor system could be involved in the control of several functions and processes. Although its role and properties are still under active investigation, it is clear that the N/OFQ–NOP receptor system regulates a wide range of biological functions including cough, urinary incontinence, anxiety and mood, pain, stress, feeding, learning and memory, locomotor activity, substance abuse, cardiovascular functions, and Parkinson's disease.^{7–12}

The complex pharmacological effects of NOP are distinct from the classical opioid receptors. N/OFQ showed sequence similarity with classical opioid peptides but interestingly it does not interact with classical opioid receptors (δ , κ , and μ). Moreover the opioid peptides have no or very low affinity for the NOP receptor. Similarly, the NOP receptor shared a high structural homology (47% overall homology, 65% homology in the trans-membrane domains) with the three classical opioid receptors; but NOP is insensitive to most of the morphine-like ligands such as naloxone. However, several known small molecules

active as central nervous system drugs showed good affinity for the NOP receptor.¹³

Identification of the essential chemical features responsible for NOP affinity may lead to the development of new small-molecule NOP ligands. NOP agonists are being investigated as potential therapeutics for anxiety, cough, and drug abuse. NOP antagonists have been studied for their utility in treating Parkinson's, depression, obesity and learning deficits.^{14,15}

Among the neuroleptics tested, spiroxatrine (**1**) (Fig. 1), an α_2 adrenergic and 5-HT_{1A} antagonist, displayed a notable affinity for NOP.^{13,14,16}

On the basis of these results, spiroxatrine was selected as the lead compound for the design of new potential NOP ligands by several research groups.^{17,18}

In particular, the 1-phenyl-1,3,8-triazaspiro[4.5]decan-4-one portion of **1**, due to its chemical features, was found to be responsible for the binding affinity of this class of compounds.¹⁷ The resulting spiropiperidine analogues exhibited high affinity for the NOP receptor. In particular, the spiropiperidine series developed by Roche and Pfizer demonstrated high affinity associated with moderate selectivity for the NOP receptor.¹⁵

Herein we report the results of the SAR study aimed at identifying a series of triazaspirodecanone derivatives as NOP receptor ligands. In particular, the SAR development plan was to

^aDepartment of Life Sciences, University of Modena & Reggio Emilia, Via G. Campi 183, 41125 Modena, Italy. E-mail: livio.brasili@unimore.it; Fax: +39 0592055131; Tel: +39 0592055139

^bDepartment of Chemical and Geological Sciences, University of Modena & Reggio Emilia, Via G. Campi 183, 41125 Modena, Italy

^cDepartment of Medical Sciences, Section of Pharmacology and National Institute of Neuroscience, University of Ferrara, Via Fossato di Mortara, 64/B, 44121 Ferrara, Italy

† Electronic supplementary information (ESI) available: Characterization of all compounds, crystallographic data, and computational methods. See DOI: 10.1039/c4md00082j

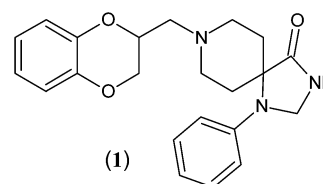


Fig. 1 Spiroxatrine (**1**).

investigate possible substitutions of the chromane core of 8-(chroman-4-yl)-1-phenyl-1,3,8-triazaspiro[4.5]decan-4-one. This compound appeared previously in a Hoffmann-La Roche patent; however no data regarding its binding affinity and activity were reported.¹⁹ Moreover, we developed a useful method to obtain single enantiomers for this class of compounds. The method was applied to 8-(chroman-4-yl)-1-phenyl-1,3,8-triazaspiro[4.5]decan-4-one and single enantiomers were separated and tested, highlighting a good enantioselective interaction with the NOP receptor. Docking studies were also performed on the NOP receptor in order to identify possible stereoselective interactions of these ligands.

Results and discussion

Chemistry

A synthetic approach different from the reductive amination, previously reported for these compounds, was employed in an attempt to increase the reaction yield and to avoid highly toxic reagents (*e.g.* cyanoborohydride).¹⁹ As described in Scheme 1, the commercially available 1-phenyl-1,3,8-triazaspiro[4.5]decan-4-one, **2**, was alkylated in the presence of various benzyl halides to produce **3**, where the benzyl halides consist of chromanyl analogues. The halides were generated *via* treatment of the corresponding alcohols with SOCl₂ as described in Scheme 1.

Similarly, the alcohols were generated by NaBH₄ reduction from the corresponding chromane analogues (Scheme 1). The required chromane derivatives were prepared as described in Scheme 2 by condensation of 2'-hydroxyacetophenone with an appropriate ketone or aldehyde.²⁰

The corresponding 3,3-dimethylchromane derivative (**17a**) was obtained by alkylation of compound **4a** (Scheme 3).²¹

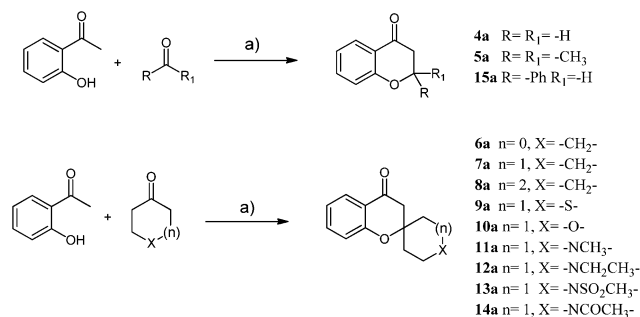
Differently the 5-fluoro analogue of **4a** was synthesized as outlined in Scheme 4.²²

Compound **16** was obtained by basic hydrolysis of the acetyl group of the triazaspirodecanone derivative **14** (Scheme 5).

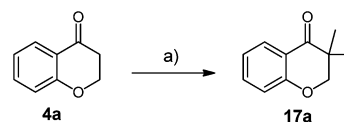
All compounds were fully characterized and the final spiro piperidine derivatives were converted into the corresponding salts with oxalic acid.

In vitro activity at human recombinant NOP receptors

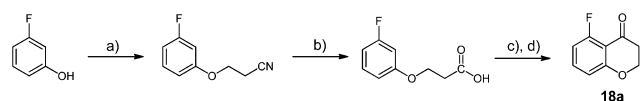
The compounds described were evaluated by measuring calcium mobilization in CHO_{NOP} cells, stably expressing the Gα_{q15} chimeric protein that forces the receptor to couple with



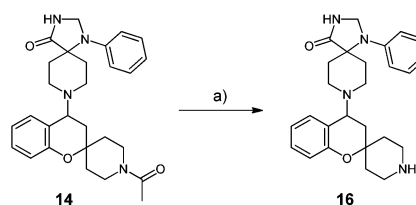
Scheme 2 Synthesis of 4-chromanone derivatives. Reagents and conditions: (a) pyrrolidine, EtOH, reflux.



Scheme 3 Synthesis of **17a**. Reagents and conditions: (a) CH₃I, KOtBu, THF, -70 °C.

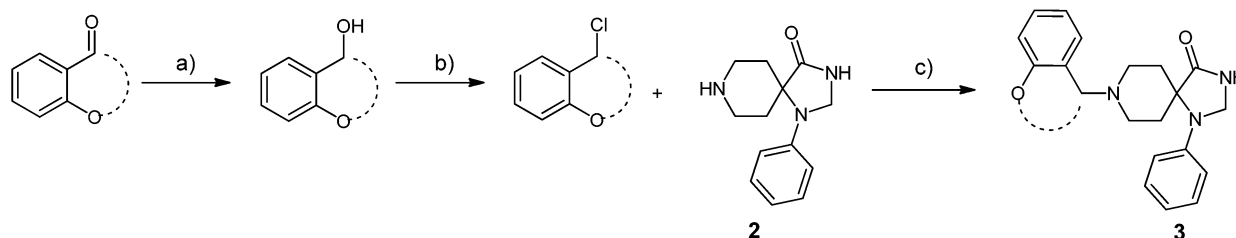


Scheme 4 Synthesis of **18a**. Reagents and conditions: (a) acrylonitrile, Triton B, 70 °C; (b) HCl conc., 100 °C; (c) SOCl₂, toluene, 0 °C to r.t.; (d) triflic acid, CH₂Cl₂, -70 °C to r.t.



Scheme 5 Synthesis of **16**. Reagents and conditions: (a) NaOH 10%, MeOH, 80 °C.

calcium signaling. This assay has been previously validated by studying the effects of a large series of standard NOP receptor ligands encompassing full and partial agonist as well as antagonist activities and of novel NOP ligands including the



Scheme 1 Synthesis of triazaspirodecanone derivatives. Reagents and conditions: (a) NaBH₄, MeOH, 0 °C; (b) SOCl₂, CH₂Cl₂, 0 °C; (c) K₂CO₃, KI, CH₃CN, reflux.

antagonists C-24, C-35 and the mixed NOP/opioid receptor agonist [Dmt¹]N/OFQ(1–13)-NH₂.^{23–26}

The novel compounds were evaluated as NOP receptor agonists using N/OFQ as the standard (Fig. 2, left panel). Under the present experimental conditions, N/OFQ produced a concentration-dependent stimulation of calcium mobilization with a pEC₅₀ of 9.68 and maximal effect of 254 ± 16% over the basal value. These results are close to those previously published.^{23,24} Results obtained with the novel compounds are summarized in Table 1. Spiroaxtrine (**1**), taken as the lead compound for this study, behaved as a low potency NOP full agonist with a pEC₅₀ of 6.49. Compounds **4** and **18** produced a concentration-dependent calcium mobilization with pEC₅₀ values of 6.80 and 6.37, respectively.

The maximal effects elicited by the compounds were not significantly different from that of N/OFQ (Table 1). However, the potency of these compounds was significantly lower than that produced by the standard agonist N/OFQ. The same compounds were found to be inactive up to 10 μM when evaluated in CHO cells expressing the Gα_{q15} protein, but not the NOP receptor, indicating that the observed stimulation of calcium mobilization is exclusively due to their ability to bind and activate the NOP receptor.

Compounds **5–10**, **13–15** and **17** produced a weak stimulation of the NOP receptor, generating incomplete concentration response curves. Thus these molecules behaved as very low potency NOP agonists. Differently, compounds **11**, **12** and **16** did not stimulate calcium mobilization up to 10 μM.

These compounds were further evaluated in antagonist-type experiments. In these studies SB-612111 was used as a positive control. Inhibition response curves were performed against a fixed concentration of N/OFQ, approximately corresponding to its EC₈₀. As shown in Fig. 2, right panel, under the present experimental conditions SB-612111 elicited a complete and concentration-dependent inhibition of the N/OFQ stimulatory effect, with a pK_B value of 8.10. This value is in line with previously reported findings.^{23,27,28} Compounds **11**, **12**, and **16** up to 10 μM did not modify the stimulatory effect of N/OFQ. In addition, compounds **7** and **13**, which displayed a weak stimulatory effect only at 10 μM, were also evaluated as NOP antagonists up to 1 μM. These compounds produced a weak inhibitory effect only at the highest concentration tested.

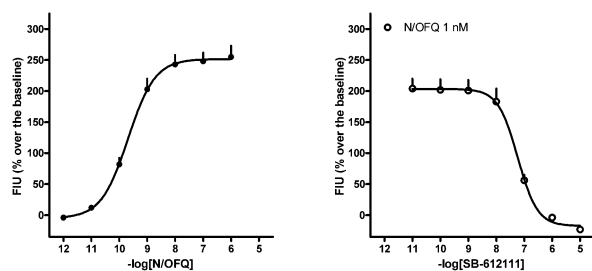


Fig. 2 Calcium mobilization experiments performed in CHO_{NOP} cells stably expressing the Gα_{q15} protein. Concentration response curve to N/OFQ (left panel) and inhibition response curve to SB-612111 vs. 1 nM N/OFQ (right panel). Data are the mean ± sem of at least 4 separate experiments performed in duplicate.

Table 1 Effects of standard and novel ligands in calcium mobilization experiments performed in CHO cells coexpressing the human NOP receptor and the Gα_{q15} chimeric protein^a

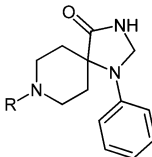
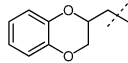
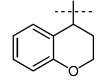
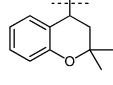
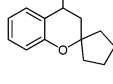
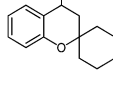
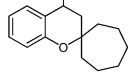
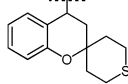
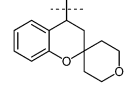
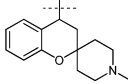
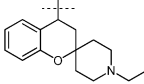
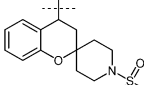
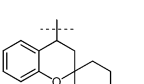
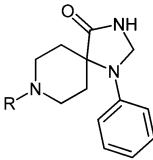
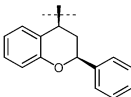
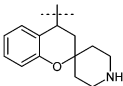
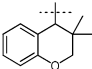
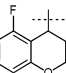
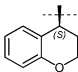
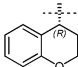
				
		Agonist		Antagonist
Compound		pEC ₅₀ (CL _{95%})	α ± SEM	pK _B (CL _{95%})
N/OFQ		9.68 (9.59–9.78)	1.00	n.d.
SB-612111		Inactive		8.10 (7.95–8.24)
1		6.49 (5.95–7.03)	0.81 ± 0.03	n.d.
4		6.80 (5.79–7.63)	1.02 ± 0.04	n.d.
5		Crc incomplete		n.d.
6		Crc incomplete		n.d.
7		Crc incomplete		<6
8		Crc incomplete		n.d.
9		Crc incomplete		n.d.
10		Crc incomplete		n.d.
11		Inactive		Inactive
12		Inactive		Inactive
13		Crc incomplete		<6
14		Crc incomplete		n.d.

Table 1 (Contd.)

			
	Agonist		Antagonist
Compound	pEC₅₀ (CL_{95%})	α ± SEM	pK_B (CL_{95%})
N/OFQ	9.68 (9.59–9.78)	1.00	n.d.
SB-612111	Inactive		8.10 (7.95–8.24)

15		Crc incomplete	n.d.	
16		Inactive	Inactive	
17		Crc incomplete	n.d.	
18		6.37 (6.31–6.43)	1.00 ± 0.09	n.d.
S-4		6.68 (6.57–6.80)	0.95 ± 0.04	n.d.
R-4		7.34 (7.29–7.39)	0.98 ± 0.04	n.d.

^a Data are mean of at least 3 separate experiments performed in duplicate. n.d.: not determined. Inactive: inactive up to 10 μM . Crc incomplete: the concentration response curve could not be completed because of the low potency of the agonist. <6: the pK_B could not be precisely determined because the ligand produced a weak inhibitory effect only at the highest concentration tested, i.e. 1 μM .

Structure–activity relationships of the NOP receptor ligands

Introduction of the chromane core on the piperidine nitrogen of 1-phenyl-1,3,8-triazaspiro[4.5]decan-4-one, as in compound **4**, moderately increases the agonist activity with respect to **1**. Introduction of a halogen atom at position 5 of compound **4**, to give **18**, leads to a slight decrease in potency. The presence of a steric hindrance at position 3 of the chromane moiety as in compound **17** decreases the ligand potency. A similar trend was observed for the introduction of alkyl and aromatic substituents on position 2 of the chromane as in compounds **5** and **15**. Anyway since recent studies suggested that the complementary lipophilic binding pocket in the NOP receptor should be able to accommodate even bigger substituents, we decided to increase the steric hindrance at position 2 of the chromane core. In fact several most active agonists or antagonists of the NOP receptor bear a tricyclic fused ring system. Thus we hypothesized that the

introduction of a third cycle could lead to an increase in activity through additional interactions. However, this strategy was not successful and compounds **6** and **15** did not show promising activity, suggesting very low steric tolerance on the chromane ring. Interestingly, homologation of the spiro structure of **6**, to give **7**, seems to convert the compound into a weak antagonist. However, the very low potency of this compound does not allow a detailed characterization of its pharmacological activity. Further homologation of the spiro alkyl substituents (**8**) led to a decrease in activity both as agonist and antagonist. The same behaviour was observed for the isomers of **7**, compounds **9**, **10** and **16**. Indeed the latter was completely inactive as its methyl and ethyl derivatives (**11** and **12**, respectively), probably because at physiological pH the nitrogen atom is protonated and the positive charge may negatively interfere with the binding process. Compound **13**, with a non-protonable sulfonamidic nitrogen which also carries the hindered substituent such as the methanesulfonyl group, showed a weak antagonist activity similar to compound **7**. However, this is not observed with compound **14** which has a similar nitrogen atom (acetamidic), indicating the relevant and discriminating role of steric interactions in the antagonist activity.

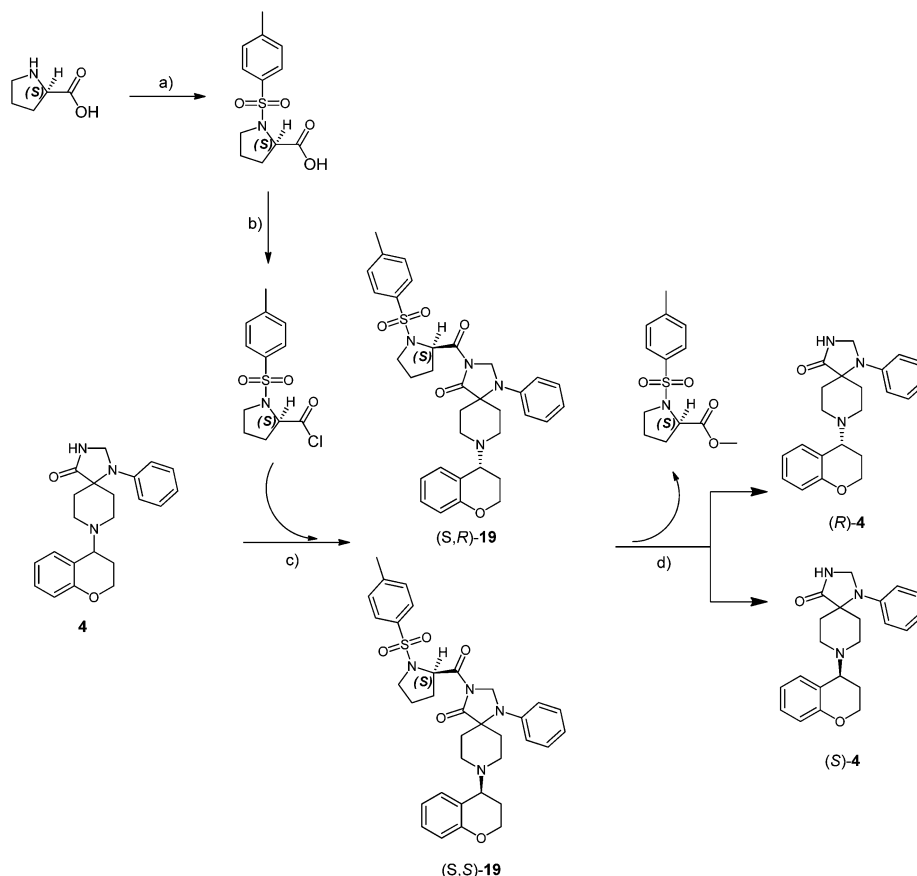
Synthesis and biological evaluation of (*S*)-**4** and (*R*)-**4**

Since previous studies suggested that chiral spiropiperidine derivatives display a stereoselective pharmacological action on NOP receptors, it was important to evaluate the activity of single stereoisomers of **4**, the most active compound of this series.²⁹

Initial attempts at fractional crystallization of the racemic (\pm)-**4** in the presence of (L)(+)-tartaric or (D)(–)-mandelic acids as resolving agents were performed with no success. Moreover the use of semi-preparative chiral HPLC gave no results since a baseline resolution was not achieved. For these reasons we were prompt to develop a new synthetic pathway to obtain single enantiomers. Resolution of (\pm)-**4** was achieved by conversion of the two enantiomers into their diastereomeric amide derivatives (*S,S*)-**19** and (*S,R*)-**19** using *N*-tosyl-(*S*)-prolyl chloride as the optically active resolving agent (Scheme 6).³⁰ *N*-Tosyl-(*S*)-prolyl chloride was previously obtained by *N*-tosylation of (*S*)-proline, followed by the formation of the acyl chloride derivative (Scheme 6).³⁰ The epimers (*S,S*)-**19** and (*S,R*)-**19** were separated by flash chromatography and then individually deprotected to yield (*S*)-**4** and (*R*)-**4** by hydrolysis with sodium methoxide. The optical rotatory power of the single stereoisomer was recorded, confirming their stereochemical purity ($R[\alpha]_D^{20} = +42.6^\circ$; $S[\alpha]_D^{20} = -41.6^\circ$).

The absolute configuration of the enantiomers was determined for the corresponding hydrogenoxalate hemihydrate salts $4 \cdot \text{H}_2\text{C}_2\text{O}_4 \cdot 1/2\text{H}_2\text{O}$. X-ray diffraction assigned to the dextrorotatory enantiomer the *R* configuration (Fig. 3).

Subsequently, the single enantiomers were evaluated as hydrogenoxalate as NOP agonists as described above. (+)-(*R*)-**4** and (–)-(*S*)-**4** produced a concentration-dependent calcium mobilization with pEC₅₀ values of 7.34 and 6.68, respectively (Table 1 and Fig. 4). Thus the results identified the (*R*)-enantiomer as the most active component possessing an activity



Scheme 6 Synthesis of *R*-4 and *S*-4. Reagents and conditions: (a) TsCl, Na₂CO₃, H₂O, r.t.; (b) SOCl₂, toluene, reflux; (c) Et₃N, CH₂Cl₂, reflux; (d) NaOMe, MeOH, r.t.

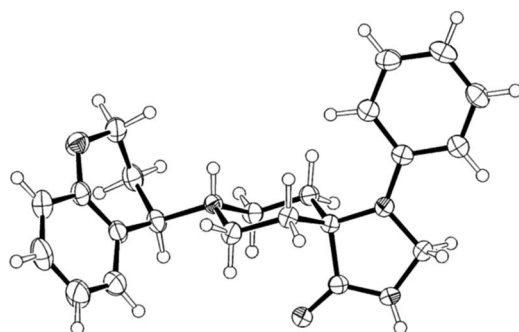


Fig. 3 X-ray structure of one of the crystallographically independent (+)-*R*-4 molecules (protonated on the piperidine nitrogen atom) in (+)-*R*-4·H₂C₂O₄·1/2H₂O. Thermal ellipsoids are drawn at 50% probability. Cutout ellipsoids are shown for nitrogen and oxygen atoms. Hydrogen atoms are represented as spheres of arbitrary radius.

5-fold higher than the (*S*)-enantiomer. Moreover, in order to demonstrate the involvement of the NOP receptor in the biological action of (+)-*R*-4 and (–)-*S*-4, inhibition response experiments were performed by testing increasing concentrations of SB-612111 against fixed concentrations of (+)-*R*-4 and (–)-*S*-4 (1 μM), approximately corresponding to their EC₈₀.

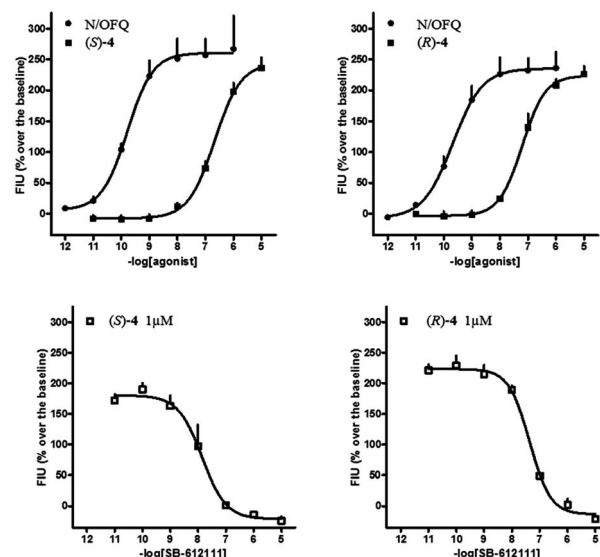


Fig. 4 Calcium mobilization experiments were performed in CHO_{NOP} cells stably expressing the Gα_{q15} protein. Top panels display the concentration response curves to N/OFQ and (S)-4 (left) or (R)-4 (right). Bottom panels show the inhibition response curves to SB-612111 vs. 1 μM (S)-4 (left) and 1 μM (R)-4 (right). Data are mean ± sem of at least 4 separate experiments performed in duplicate.

The pK_B values obtained for SB-612111 vs. (+)-(*R*)-4 and (–)-(*S*)-4 were 8.67 and 8.58, respectively (Fig. 4B), indicating that the latter compounds behaved as full agonists interacting with the NOP receptor at the orthosteric binding site.

Docking studies

In order to understand possible stereospecific interactions of (+)-(*R*)-4 and (–)-(*S*)-4 docking studies were performed. Taking advantage of the crystal structure of the NOP receptor (PDB code 4EA3), recently published by Thompson *et al.*, Molegro Virtual Docker (MVD) software was applied to dock (+)-(*R*)-4 and (–)-(*S*)-4 within the binding pocket of the NOP receptor.³¹ It should be emphasized that the crystal structure of the NOP receptor has been solved in complex with an antagonist (C-24) and thus represents the inactive form of the receptor. Thus caution

should be exercised while using such structures for studying the docking of a receptor agonist. However, recent findings obtained by comparing the few examples of the structure of the same GPCR in complex with an agonist or with an antagonist demonstrated that the agonist bound form of the receptor showed relatively minor backbone deviations compared to the antagonist bound form, allowing the initial docking of agonists into such model.³² Substantial conformational changes, particularly in the cytoplasmic ends of helices V and VI, are observed only when the agonist bound receptor is crystallized together with the G protein.³³

The software MVD was initially evaluated on the peptide mimetic antagonist C-24 to verify whether the docking method can reproduce the crystal binding model. The average root-mean-square distance (rmsd) of the best ranking pose of the compound as compared to its binding pose in the respective crystal structure was found to be 0.68 Å, proving that MVD is able to accurately dock this type of compound (see the ESI†). The crystal structure obtained for the *R* stereoisomer was employed as an input file to build the ligand with Spartan'08. The docking output clearly indicates a similar binding mode for (+)-(*R*)-4 and (–)-(*S*)-4 (Fig. 5 and 6). In particular, two hydrophilic interactions were observed: the salt bridge between the protonated piperidine nitrogen and Asp-130, an H-bond between the amide nitrogen of the agonist and the oxygen of Thr-305 (Fig. 6).

These polar interactions are probably essential for the activity, playing a crucial role in anchoring the ligand to the binding site. Moreover, the benzopyran moiety is accommodated within the lipophilic cavity lined by Ile-127, Tyr-131, Phe-135, Ile-204, Phe-215, Ile-219, Phe-220, Phe-224, Phe-272, Trp-276, Val-279, and Val-283, further stabilizing the compound in the binding pocket by multiple interactions. The main difference observed in the binding mode of the two stereoisomers is

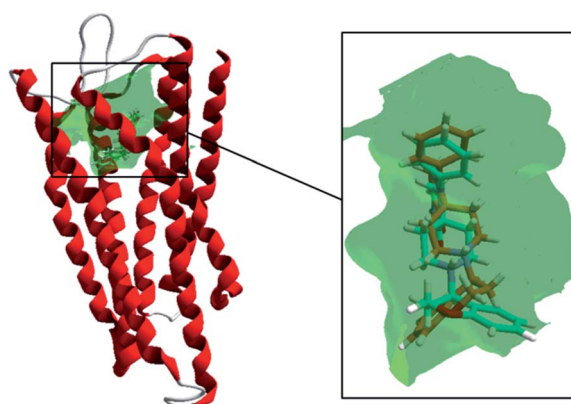


Fig. 5 Cartoon representation of the NOP crystal structure with its ligand-binding pocket shown as a green transparent surface. The best results obtained from docking output for (*S*)-4 (orange) and (*R*)-4 (blue) are reported within the binding pocket.

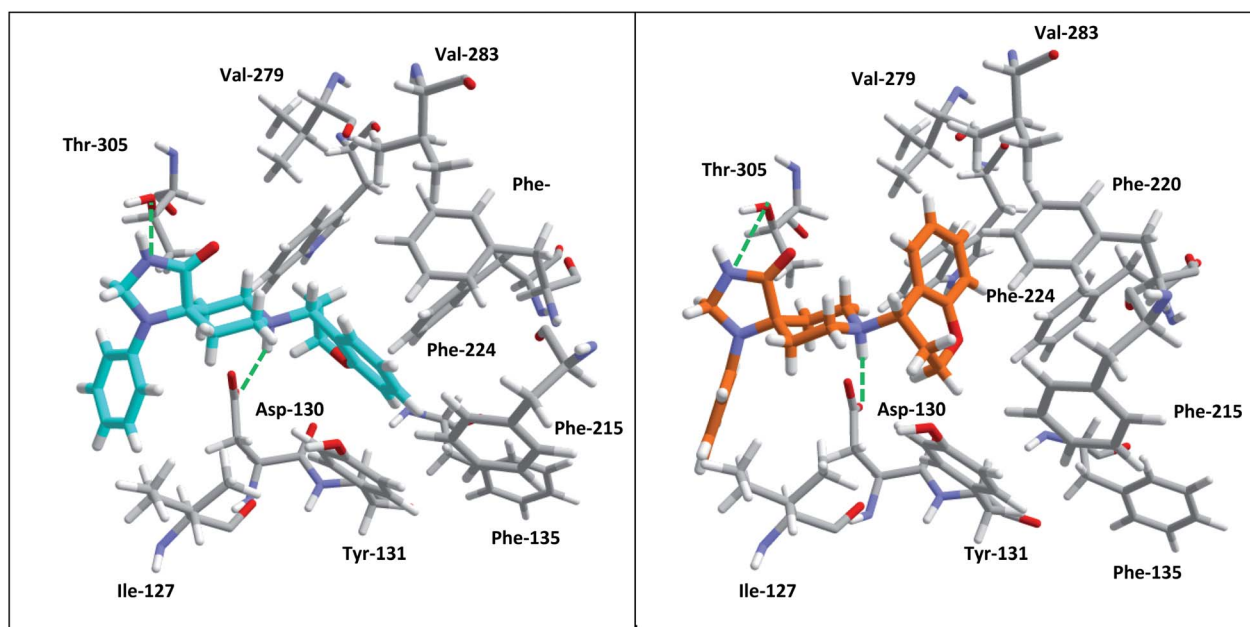


Fig. 6 Binding mode of (*R*)-4 (blue, left panel) and (*S*)-4 (orange, right panel). Polar interactions are indicated with green dashes.

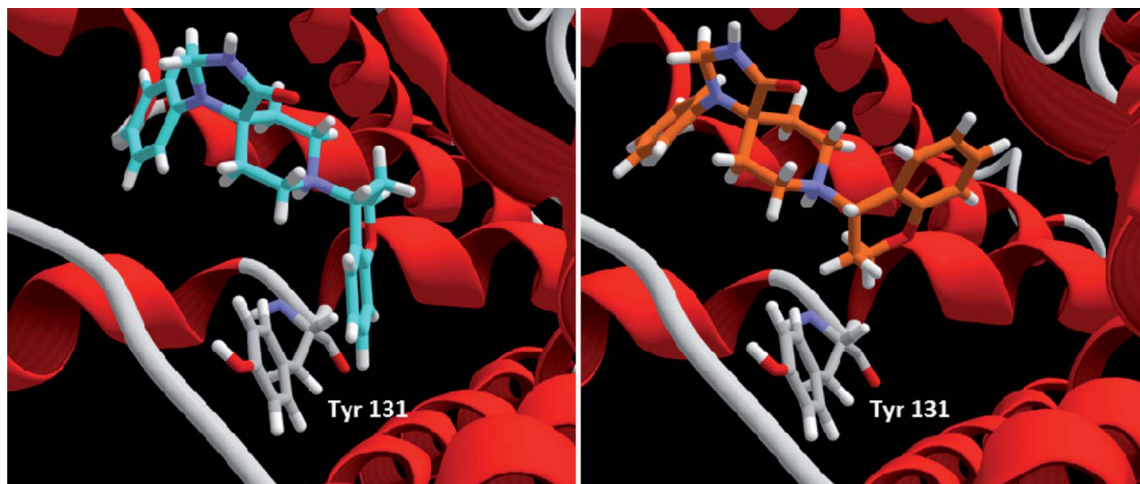


Fig. 7 Aromatic ring of (*R*)-4 (blue, left panel) strongly interacts with Tyr-131 and aromatic ring of (*S*)-4 (orange, right panel) lined opposite to the Tyr-131 residue.

the interaction with Tyr-131 (Fig. 7). As described by Thompson *et al.*, point mutation of this residue with alanine residue had a deleterious effect on agonist potency suggesting that Tyr-131 participates in crucial π -stacking interactions.^{31,34}

Experimental section

Chemistry

Materials and methods. All reagents, solvents and other chemicals were used as purchased from Sigma-Aldrich without further purification unless otherwise specified. Air- or moisture-sensitive reactants and solvents were employed in reactions carried out under a nitrogen atmosphere unless otherwise noted. Flash column chromatography purifications (medium pressure liquid chromatography) were carried out using Merck silica gel 60 (230–400 mesh, ASTM). The purity of the compounds was determined by elemental analysis (C, H, N) that was performed on a Carlo Erba 1106 Analyzer in the Microanalysis Laboratory of the Life Sciences Department of Università degli Studi di Modena e Reggio Emilia and the results reported here are within $\pm 0.4\%$ of the theoretical values. Melting points were determined with a Stuart SMP3 and they are uncorrected. The structures of all isolated compounds were ensured by nuclear magnetic resonance (NMR) and mass spectrometry. ^1H and ^{13}C NMR (1D and 2D experiments) spectra were recorded on a DPX-200 Avance (Bruker) spectrometer at 200 MHz and on a DPX-400 Avance (Bruker) spectrometer at 400 MHz. Chemical shifts are expressed in δ (ppm). ^1H NMR chemical shifts are relative to tetramethylsilane (TMS) as internal standard. ^{13}C NMR chemical shifts are relative to TMS at δ 0.0 or to the ^{13}C signal of the solvent: CDCl_3 δ 77.04, CD_3OD δ 49.8, $\text{DMSO}-d_6$ δ 39.5. NMR data are reported as follows: chemical shift, number of protons/carbons, multiplicity (s, singlet; d, doublet; t, triplet; q, quartet; m, multiplet; br, broadened), coupling constants (Hz) and assignment (chrom. = chromane, cyclophen. = spirocyclopentane, cyclohex. = spirocyclohexane, cyclohep.

= spirocycloheptane, pipd. = spiropiperidine, phen. = phenyl, tasd = 1-phenyl-1,3,8-triazaspiro[4.5]decan-4-one, arom. tasd = aromatic portion of 1-phenyl-1,3,8-triazaspiro[4.5]decan-4-one, Tos-pro = tosylproline, arom. Tos-pro = aromatic portion of tosylproline). ^1H - ^1H correlation spectroscopy (COSY), ^1H - ^{13}C heteronuclear multiple quantum coherence (HMQC) and heteronuclear multiple bond connectivity (HMBC) experiments were performed for the determination of ^1H - ^1H and ^1H - ^{13}C correlations, respectively. Mass spectra were obtained on a hybrid QTOF mass spectrometer (PE SCIEX-QSTAR) using electrospray ionization mode (HR-ESI-MS, ion voltage of 4800 V). The HPLC experimental conditions of the HPLC-MS system are as follows: flow rate 5 ml min^{-1} , sample solution (10 pmol ml^{-1}) of the selected compound with 0.1% acetic acid, mobile phase consisting of methanol (50%) and water (50%).

The oxalate salts of all tested compounds were used for pharmacological evaluations.

General procedure A

A solution of 2'-hydroxyacetophenone (1.0 mmol) and the selected ketone/aldehyde (1.5 mmol) in EtOH was treated with pyrrolidine (1.5 mmol) and then heated at reflux for 24 h. After completion (monitored by TLC), the reaction mixture was concentrated *in vacuo*. The residue was dissolved in EtOAc and washed with HCl 1 N and brine. The organic layer was dried on anhydrous Na_2SO_4 , filtered, and evaporated *in vacuo*. Purification by flash column chromatography gave the desired compound.

2,3-Dihydro-4H-chromen-4-one (4a). The compound was obtained from paraformaldehyde following the general procedure A as a white solid (95% yield).

Mp: 41–42 °C; ^1H NMR (200 MHz, CDCl_3): δ = 2.82 (t, J = 6.5 Hz, 2H, CH_2 -3 chrom.), 4.54 (t, J = 6.5 Hz, 2H, CH_2 -2 chrom.), 6.96–7.05 (m, 2H, CH-6, CH-8 chrom.), 7.45–7.48 (m, 1H, CH-7 chrom.), 7.90 ppm (dd, J = 8.1, 1.5 Hz, 1H, CH-5 chrom.)

General procedure B

The selected ketone (1.0 mmol) was suspended in methanol (10 ml) and treated with an excess of NaBH₄ (1.5 mmol) at 0 °C. The resulting mixture was stirred for 30 minutes at room temperature, then concentrated *in vacuo*. The residue was partitioned between CH₂Cl₂ and H₂O. The organic layer was separated, and the aqueous layer was extracted with CH₂Cl₂. The organic layers were then combined, washed with H₂O, dried over anhydrous Na₂SO₄, filtered, and concentrated *in vacuo* to yield the desired compound.

3,4-Dihydro-2H-chromen-4-ol (4b). The compound was obtained from **4a** following the general procedure B as an oil (94% yield).

¹H NMR (200 MHz, CDCl₃): δ = 1.87 (dd, *J* = 4.7 Hz, 1H, –OH), 1.95–2.26 (m, 2H, CH₂-3 chrom.), 4.18–4.38 (m, 2H, CH₂-2 chrom.), 4.79 (dd, *J* = 4.1, 8.3 Hz, 1H, CH-4 chrom.), 6.79–7.00 (m, 2H, CH-6, CH-8 chrom.), 7.13–7.37 ppm (m, 2H, CH-5, CH-7 chrom.)

General procedure C

To an ice-bath cooled solution of the selected alcohol derivative (1.0 mmol) in CH₂Cl₂ (10 ml), thionyl chloride (1.5 mmol) was added dropwise. The reaction mixture was stirred at room temperature for 1 h then water was added. The aqueous layer was decanted, separated and then extracted two times with CH₂Cl₂. The organic layers were combined, washed with H₂O, dried over anhydrous Na₂SO₄, filtered, and concentrated *in vacuo* to yield the desired compound.

4-Chloro-3,4-dihydro-2H-chromene (4c). The compound was obtained from **4b** following the general procedure C as a black oil (70% yield).

¹H NMR (200 MHz, CDCl₃): δ = 2.15–2.34 (m, 1H, CHa-3 chrom.), 2.39–2.63 (m, 1H, CHb-3 chrom.), 4.20–4.59 (m, 2H, CH₂-2 chrom.), 5.24 (m, 1H, CH-4 chrom.), 6.70–7.03 (m, 2H, CH-6, CH-8 chrom.), 7.07–7.40 ppm (m, 2H, H-5, CH-7 chrom.)

General procedure D

To a solution of 1-phenyl-1,3,8-triazaspiro[4.5]decan-4-one (1.5 mmol), K₂CO₃ (3.0 mmol), KI (1.0 mmol) in anhydrous acetonitrile (10 ml) was added the selected benzyl chloride (1.0 mmol) portionwise. The resulting mixture was stirred under reflux for 4 h, then cooled to room temperature and concentrated *in vacuo*. The residue was partitioned between EtOAc and H₂O. The organic layer was separated, and the aqueous layer was extracted with EtOAc. The organic layers were combined, washed with H₂O, dried over anhydrous Na₂SO₄, filtered, and concentrated *in vacuo*. The residue was purified by flash chromatography to yield the desired compound.

8-(Chroman-4-yl)-1-phenyl-1,3,8-triazaspiro[4.5]decan-4-one (4). The compound was obtained from **4c** following the general procedure D as a white solid (48% yield).

Mp: 210–211 °C; ¹H NMR (400 MHz, CDCl₃): δ = 1.63 (m, 1H, CHa-6/CHa-10 *tasd*), 1.78 (m, 1H, CHa-6/CHa-10 *tasd*), 1.97–2.02 (m, 1H, CHa-3 chrom.), 2.08–2.17 (m, 1H, CHb-3 chrom.), 2.56–2.64 (m, 2H, CHb-6/CHb-10 *tasd*, CHa-7/CHa-9 *tasd*), 2.80–

2.88 (m, 3H, CHb-6/CHb-10 *tasd*, CHa-7/CHa-9 *tasd*, CHb-7/CHb-9 *tasd*), 3.29–3.36 (m, 1H, CHb-7/CHb-9 *tasd*), 3.95 (dd, *J* = 5.5, 9.0 Hz, 1H, CH-4 chrom.), 4.11–4.16 (m, 1H, CHa-2 chrom.), 4.34–4.39 (m, 1H, CHb-2 chrom.), 4.72 (q, *J* = 4.2 Hz, 2H, CH₂-2 *tasd*), 6.77 (dd, *J* = 0.8, 8.2 Hz, 1H, CH-8 chrom.), 6.85 (t, *J* = 7.3 Hz, 1H, CH-4 arom. *tasd*), 6.90 (ddd, *J* = 0.8, 7.7, 8.2 Hz, 1H, CH-6 chrom.), 6.94 (d, *J* = 8.1 Hz, 2H, CH-2, CH-6 arom. *tasd*), 7.11 (ddd, *J* = 1.2, 7.7, 8.2 Hz, 1H, CH-7 chrom.), 7.27 (s, 1H, NH), 7.33 (dd, *J* = 7.5, 8.5 Hz, 2H, CH-3, CH-5 arom. *tasd*), 7.59 ppm (d, *J* = 7.7 Hz, 1H, CH-5 chrom.); ¹³C NMR (400 MHz, CDCl₃): δ = 21.3 (C-3 chrom.), 29.1 (C-6/C-10 *tasd*), 29.5 (C-6/C-10 *tasd*), 42.3 (C-7/C-9 *tasd*), 47.9 (C-7/C-9 *tasd*), 58.6 (C-4 chrom.), 59.0 (C-2 *tasd*), 59.1 (C-5 *tasd*), 65.0 (C-2 chrom.), 114.4 (C-2, C-6 arom. *tasd*), 116.4 (C-8 chrom.), 118.2 (C-4 arom. *tasd*), 120.0 (C-6 chrom.), 123.7 (C-4a chrom.), 127.9 (C-7 chrom.), 128.3 (C-5 chrom.), 129.0 (C-3, C-5 arom. *tasd*), 142.9 (C-1 arom. *tasd*), 155.5 (C-8a chrom.), 178.3 ppm (CO *tasd*).

The free amine was then converted to the corresponding hydroxoxalate from acetone.

Mp: 178–182 °C; ¹H NMR (200 MHz, DMSO): δ = 1.80–1.86 (m, 2H, CHa-6/CHa-10 *tasd*), 2.21–2.32 (m, 2H, CH₂-3 chrom.), 2.55–2.91 (m, 2H, CHa-6/CHa-10 *tasd*), 3.05–3.15 (m, 1H, CHa-7/CHa-9 *tasd*), 3.26–2.31 (m, 1H, CHa-7/CHa-9 *tasd*), 3.43–3.51 (m, 1H, CHb-7/CHb-9 *tasd*), 3.69–3.82 (m, 1H, CHb-7/CHb-9 *tasd*), 4.18–4.23 (m, 1H, CHa-2 chrom.), 4.35–4.43 (m, 1H, CHb-2 chrom.), 4.56–4.62 (m, 3H, CH₂-2 *tasd*, CH-4 chrom.), 6.75–7.00 (m, 5H, CH-2, CH-4, CH-6 arom. *tasd*; C-6, C-8 chrom.), 7.25 (m, 3H, CH-3, CH-5 arom. *tasd*; CH-7 chrom.), 7.55 (d, *J* = 7.5 Hz, 1H, CH-5 chrom.), 8.86 ppm (s, 1H, oxalic acid).

HRMS-ESI *m/z* [M + H]⁺ calc. for C₂₂H₂₆N₃O₂: 364.2026; found: 364.2029; anal. calcd for C₂₄H₂₇N₃O₆: C, 63.56; H, 6.00; N, 9.27; found C, 63.71; H, 6.15; N, 9.41.

N-Tosyl-(S)-prolyl chloride. To a solution of (S)-proline (1 g, 8.7 mmol) in 7.5 ml of water was added Na₂CO₃ (1.70 g, 16.0 mmol) and then *p*-toluenesulfonyl chloride (2.00 g, 10.5 mmol) was added slowly at 0 °C. The reaction mixture was stirred at room temperature overnight. HCl 1 N was added until the solution was acidic and the resulting mixture was taken up in ethyl acetate (4 × 15 ml). The organic phase was dried over Na₂SO₄ and filtered, and the solvent was evaporated. The product (N-tosyl-(S)-proline) was obtained in 78% yield and used for the next step. N-Tosyl-(S)-proline (1 g, 3.5 mmol) was dissolved in 6 ml of toluene; to this solution was carefully added thionyl chloride (1.32 g, 11.1 mmol). The reaction mixture was refluxed for 30 min. After removal of the solvent, 0.98 g (3.4 mmol, 97% yield) of N-tosyl-(S)-prolyl chloride were obtained and it was immediately used for the next step without further purification.

Mp: 56–57 °C; ¹H NMR (400 MHz, CDCl₃): δ = 1.84–1.90 (m, 1H, CHa-4 Tos-pro), 1.92–2.05 (m, CHb-4, CHa-3 Tos-pro), 2.15–2.23 (m, 1H, CHb-3 Tos-pro), 2.48 (s, 3H, CH₃ Tos-pro), 3.35–3.45 (m, 1H, CHa-5 Tos-pro), 3.50–3.56 (m, 1H, CHb-5 Tos-pro), 4.65 (dd, *J* = 6.1, 7.9 Hz, 1H, CH-2 Tos-pro), 7.37 (d, *J* = 8.0 Hz, 2H, CH-3, CH-5 arom. Tos-pro), 7.78 ppm (d, *J* = 8.0 Hz, 2H, CH-2, CH-6 arom. Tos-pro).

8-(Chroman-4-yl)-1-phenyl-3-((S)-1-tosylpyrrolidine-2-carbonyl)-1,3,8-triazaspiro[4.5]decan-4-one (S,S)-(19) (S,R)-19. To a solution of (±)-**4** (0.544 g, 1.5 mmol) in CH₂Cl₂ was added triethylamine

(1.67 ml, 12 mmol) and a solution of *N*-tosyl-(*S*)-prolyl chloride (1.72 g, 6 mmol) in CH₂Cl₂ at 0 °C. The reaction was warmed to RT and refluxed for 24 min. NaHCO₃ was added and the organic layer was separated and washed with H₂O, dried over Na₂SO₄ and concentrated under reduced pressure. The residue was purified by flash chromatography (cyclohexane–EtOAc 70 : 30) to yield single diastereomers.

8-((*S*)-Chroman-4-yl)-1-phenyl-3-((*S*)-1-tosylpyrrolidine-2-carbonyl)-1,3,8-triazaspiro[4.5]decan-4-one (less polar isomer) (*S,S*)-19. The compound was obtained as a yellow solid (0.267 g, 0.435 mmol, 29% yield).

Mp: 141–142 °C; ¹H NMR (400 MHz, CDCl₃): δ = 1.87–1.93 (m, 2H, CHa-6/CHa-10 *tasd*, CHa-4 *Tos-pro*), 1.92–2.08 (m, 4H, CHa-3 *chrom.*, CHa-3 *Tos-pro*, CHb-4 *Tos-pro*, CHa-6/CHa-10 *tasd*), 2.17–2.25 (m, 1H, CHb-3 *chrom.*), 2.26–2.32 (m, 1H, CHb-3 *Tos-pro*), 2.37–2.43 (m, 1H, CHb-6/CHb-10 *tasd*), 2.48 (s, 3H, CH₃ *Tos-pro*), 2.52–2.57 (m, 1H, CHb-6/CHb-10 *tasd*), 2.66–2.73 (m, 1H, CHa-7/CHa-9 *tasd*), 2.83–2.88 (m, 2H, CHa-7/CHa-9 *tasd*, CHb-7/CHb-9 *tasd*), 3.17–3.20 (m, 1H, CHb-7/CHb-9 *tasd*), 3.30–3.38 (m, 1H, CHa-5 *Tos-pro*), 3.55–3.60 (m, 1H, CHb-5 *Tos-pro*), 4.01 (dd, *J* = 5.6, 8.1 Hz, 1H, CH-4 *chrom.*), 4.15–4.22 (m, 1H, CHa-2 *chrom.*), 4.39–4.44 (m, 1H, CHb-2 *chrom.*), 5.03 (d, *J* = 7.0 Hz, 1H, CHa-2 *tasd*), 5.13 (d, *J* = 7.0 Hz, 1H, CHb-2 *tasd*), 5.61 (dd, *J* = 3.8, 9.0 Hz, 1H, CH-2 *Tos-pro*), 6.82 (d, *J* = 8.0 Hz, 1H, CH-8 *chrom.*), 6.94 (dd, *J* = 7.3, 7.4 Hz, 1H, CH-6 *chrom.*), 7.08 (t, *J* = 7.3 Hz, 1H, CH-4 *arom. tasd*), 7.12–7.18 (m, 3H, CH-7 *chrom.*, CH-2, CH-6 *arom. tasd*), 7.36–7.42 (m, 4H, CH-3, CH-5 *arom. tasd*, CH-3, CH-5 *arom. Tos-pro*), 7.57 (d, *J* = 8.2 Hz, 1H, CH-5 *chrom.*), 7.84 ppm (d, *J* = 8.2 Hz, 2H, CH-2, CH-6 *arom. Tos-pro*).

8-((*R*)-Chroman-4-yl)-1-phenyl-3-((*S*)-1-tosylpyrrolidine-2-carbonyl)-1,3,8-triazaspiro[4.5]decan-4-one (more polar isomer) (*R,S*)-19. The compound was obtained as a yellow solid (0.396 g, 0.645 mmol, 43% yield).

Mp: 146–148 °C; ¹H NMR (400 MHz, CDCl₃): δ 1.77–1.83 (m, 2H, CHa-6/CHa-10 *tasd*, CHa-4 *Tos-pro*), 1.96–2.08 (m, 4H, CHa-3 *chrom.*, CHa-3 *Tos-pro*, CHb-4 *Tos-pro*, CHa-6/CHa-10 *tasd*), 2.17–2.25 (m, 1H, CHb-3 *chrom.*), 2.26–2.30 (m, 1H, CHb-3 *Tos-pro*), 2.31–2.34 (m, 1H, CHb-6/CHb-10 *tasd*), 2.47 (s, 3H, CH₃ *Tos-pro*), 2.52–2.58 (m, 1H, CHb-6/CHb-10 *tasd*), 2.72–2.80 (m, 2H, CHa-7/CHa-9 *tasd*, CHa-7/CHa-9 *tasd*), 2.82–2.85 (m, 1H, CHb-7/CHb-9 *tasd*), 3.22–3.27 (m, 1H, CHb-7/CHb-9 *tasd*), 3.32–3.38 (m, 1H, CHa-5 *Tos-pro*), 3.56–3.61 (m, 1H, CHb-5 *Tos-pro*), 3.99 (m, 1H, CH-4 *chrom.*), 4.15–4.22 (m, 1H, CHa-2 *chrom.*), 4.40–4.45 (m, 1H, CHb-2 *chrom.*), 5.07 (d, *J* = 7.1 Hz, 1H, CHa-2 *tasd*), 5.11 (d, *J* = 7.1 Hz, 1H, CHb-2 *tasd*), 5.58 (dd, *J* = 3.7, 8.9 Hz, 1H, CH-2 *Tos-pro*), 6.83 (d, *J* = 7.5 Hz, 1H, CH-8 *chrom.*), 6.93 (dd, *J* = 7.2, 7.4 Hz, 1H, CH-6 *chrom.*), 7.08 (t, *J* = 7.3 Hz, 1H, CH-4 *arom. tasd*), 7.12–7.18 (m, 3H, CH-7 *chrom.*, CH-2, CH-6 *arom. tasd*), 7.36–7.42 (m, 4H, CH-3, CH-5 *arom. tasd*, CH-3, CH-5 *arom. Tos-pro*), 7.55 (d, *J* = 7.1 Hz, 1H, CH-5 *chrom.*), 7.82 ppm (d, *J* = 8.2 Hz, 2H, CH-2, CH-6 *arom. Tos-pro*).

(*R*)-8-(Chroman-4-yl)-1-phenyl-1,3,8-triazaspiro[4.5]decan-4-one (+)-(*R*)-4. (*R,S*)-19 was added to a 30% (p/v) solution of sodium methoxide in methanol. The mixture was stirred at room temperature for 1 h. The solvent was evaporated and the

residue was dissolved in H₂O and extracted three times with CH₂Cl₂. The organic phase was washed with brine and dried over Na₂SO₄, and the solvent was removed under vacuum. The products were isolated without further purification (0.222 g, 0.612 mmol, 95% yield).

Mp: 210–211 °C; [α]_D²⁰ = +42.6° (15 mg ml^{−1} CH₂Cl₂); ¹H NMR (400 MHz, CDCl₃): δ = 1.63 (m, 1H, CHa-6/CHa-10 *tasd*), 1.78 (m, 1H, CHa-6/CHa-10 *tasd*), 1.97–2.02 (m, 1H, CHa-3 *chrom.*), 2.08–2.17 (m, 1H, CHb-3 *chrom.*), 2.56–2.64 (m, 2H, CHb-6/CHb-10 *tasd*, CHa-7/CHa-9 *tasd*), 2.80–2.88 (m, 3H, CHb-6/CHb-10 *tasd*, CHa-7/CHa-9 *tasd*, CHb-7/CHb-9 *tasd*), 3.29–3.36 (m, 1H, CHb-7/CHb-9 *tasd*), 3.95 (dd, *J* = 5.5, 9.0 Hz, 1H, CH-4 *chrom.*), 4.11–4.16 (m, 1H, CHa-2 *chrom.*), 4.34–4.39 (m, 1H, CHb-2 *chrom.*), 4.72 (q, *J* = 4.2 Hz, 2H, CH₂-2 *tasd*), 6.77 (dd, *J* = 0.8, 8.2 Hz, 1H, CH-8 *chrom.*), 6.85 (t, *J* = 7.3 Hz, 1H, CH-4 *arom. tasd*), 6.90 (ddd, *J* = 0.8, 7.7, 8.2 Hz, 1H, CH-6 *chrom.*), 6.94 (d, *J* = 8.1 Hz, 2H, CH-2, CH-6 *arom. tasd*), 7.11 (ddd, *J* = 1.2, 7.7, 8.2 Hz, 1H, CH-7 *chrom.*), 7.27 (bs, 1H, NH), 7.33 (dd, *J* = 7.5, 8.5 Hz, 2H, CH-3, CH-5 *arom. tasd*), 7.59 ppm (d, *J* = 7.7 Hz, 1H, CH-5 *chrom.*); ¹³C NMR (400 MHz, CDCl₃): δ = 21.3 (C-3 *chrom.*), 29.0 (C-6/C-10 *tasd*), 29.5 (C-6/C-10 *tasd*), 42.2 (C-7/C-9 *tasd*), 47.9 (C-7/C-9 *tasd*), 58.5 (C-4 *chrom.*), 59.0 (C-2 *tasd*), 59.1 (C-5 *tasd*), 65.0 (C-2 *chrom.*), 114.4 (C-2, C-6 *arom. tasd*), 116.4 (C-8 *chrom.*), 118.2 (C-4 *arom. tasd*), 120.0 (C-6 *chrom.*), 123.7 (C-4a *chrom.*), 127.8 (C-7 *chrom.*), 128.3 (C-5 *chrom.*), 129.0 (C-3, C-5 *arom. tasd*), 142.9 (C-1 *arom. tasd*), 155.5 (C-8a *chrom.*), 178.3 ppm (C=O *tasd*).

The free amine was then converted to the corresponding hydrogenoxalate hemihydrate salt (+)-*R*-4 · H₂C₂O₄ · 1/2H₂O from acetone.

Mp: 178–182 °C; ¹H-NMR (400 MHz, DMSO): δ = 1.80 (m, 2H, CHa-6/CHa-10 *tasd*), 2.21 (m, 2H, CH₂-3 *chrom.*), 2.55–2.91 (m, 2H, CHa-6/CHa-10 *tasd*), 3.05–3.10 (m, 1H, CHa-7/CHa-9 *tasd*), 3.26 (m, 1H, CHa-7/CHa-9 *tasd*), 3.43–3.50 (m, 1H, CHb-7/CHb-9 *tasd*), 3.69–3.74 (m, 1H, CHb-7/CHb-9 *tasd*), 4.18–4.22 (m, 1H, CHa-2 *chrom.*), 4.35–4.39 (m, 1H, CHb-2 *chrom.*), 4.56–4.66 (m, 3H, CH₂-2 *tasd*, CH-4 *chrom.*), 6.75–7.00 (m, 5H, CH-2, CH-4, CH-6 *arom. tasd*; CH-6, CH-8 *chrom.*), 7.25 (m, 3H, CH-3, CH-5 *arom. tasd*; CH-7 *chrom.*), 7.55 ppm (d, *J* = 7.5 Hz, 1H, CH-5 *chrom.*)

HRMS-ESI *m/z* [M + H]⁺ calc. for C₂₂H₂₆N₃O₂: 364.2019; found: 364.2018; anal. calcd for C₂₄H₂₇N₃O₆: C, 63.56; H, 6.00; N, 9.27; found C, 63.44; H, 5.91; N, 9.01.

(*S*)-8-(Chroman-4-yl)-1-phenyl-1,3,8-triazaspiro[4.5]decan-4-one (−)-(*S*)-4. (*S,S*)-19 was added to a 30% (p/v) solution of sodium methoxide in methanol. The mixture was stirred at room temperature for 1 h. The solvent was evaporated and the residue was dissolved in H₂O and extracted three times with CH₂Cl₂. The organic phase was washed with brine and dried over Na₂SO₄, and the solvent was removed under vacuum. The products were isolated without further purification (0.151 g, 0.417 mmol, 96% yield).

Mp: 210–211 °C; [α]_D²⁰ = −41.6° (16 mg ml^{−1} CH₂Cl₂); ¹H NMR (400 MHz, CDCl₃): δ = 1.63 (m, 1H, CHa-6/CHa-10 *tasd*), 1.78 (m, 1H, CHa-6/CHa-10 *tasd*), 1.97–2.02 (m, 1H, CHa-3 *chrom.*), 2.08–2.17 (m, 1H, CHb-3 *chrom.*), 2.56–2.64 (m, 2H, CHb-6/CHb-10 *tasd*, CHa-7/CHa-9 *tasd*), 2.80–2.88 (m, 3H,

CHb-6/CHb-10 tasd, CHa-7/CHa-9 tasd, CHb-7/CHb-9 tasd), 3.29–3.36 (m, 1H, CHb-7/CHb-9 tasd), 3.95 (dd, $J = 5.5, 9.0$ Hz, 1H, CH-4 chrom.), 4.11–4.16 (m, 1H, CHa-2 chrom.), 4.34–4.39 (m, 1H, CHb-2 chrom.), 4.72 (q, $J = 4.2$ Hz, 2H, CH₂-2 tasd), 6.77 (dd, $J = 0.8, 8.2$ Hz, 1H, CH-8 chrom.), 6.85 (t, $J = 7.3$ Hz, 1H, CH-4 arom. tasd), 6.90 (ddd, $J = 0.8, 7.7, 8.2$ Hz, 1H, CH-6 chrom.), 6.94 (d, $J = 8.1$ Hz, 2H, CH-2, CH-6 arom. tasd), 7.11 (ddd, $J = 1.2, 7.7, 8.2$ Hz, 1H, CH-7 chrom.), 7.27 (bs, 1H, NH), 7.33 (dd, $J = 7.5, 8.5$ Hz, 2H, CH-3, CH-5 arom. tasd), 7.59 ppm (d, $J = 7.7$ Hz, 1H, CH-5 chrom.); ¹³C NMR (400 MHz, CDCl₃): $\delta = 21.3$ (C-3 chrom.), 29.0 (C-6/C-10 tasd), 29.5 (C-6/C-10 tasd), 42.2 (C-7/C-9 tasd), 47.9 (C-7/C-9 tasd), 58.5 (C-4 chrom.), 59.0 (C-2 tasd), 59.1 (C-5 tasd), 65.0 (C-2 chrom.), 114.4 (C-2, C-6 arom. tasd), 116.4 (C-8 chrom.), 118.2 (C-4 arom. tasd), 120.0 (C-6 chrom.), 123.7 (C-4a chrom.), 127.8 (C-7 chrom.), 128.3 (C-5 chrom.), 129.0 (C-3, C-5 arom. tasd), 142.9 (C-1 arom. tasd), 155.5 (C-8a chrom.), 178.3 ppm (C=O tasd).

The free amine was then converted to the corresponding hydrogenoxalate hemihydrate salt (–)-**5**·4·H₂C₂O₄·1/2H₂O from acetone.

Mp: 178–182 °C; ¹H-NMR (400 MHz, DMSO): $\delta = 1.80$ (m, 2H, CHa-6/CHa-10 tasd), 2.21 (m, 2H, CH₂-3 chrom.), 2.55–2.91 (m, 2H, CHa-6/CHa-10 tasd), 3.05–3.10 (m, 1H, CHa-7/CHa-9 tasd), 3.26 (m, 1H, CHa-7/CHa-9 tasd), 3.43–3.50 (m, 1H, CHb-7/CHb-9 tasd), 3.69–3.74 (m, 1H, CHb-7/CHb-9 tasd), 4.18–4.22 (m, 1H, CHa-2 chrom.), 4.35–4.39 (m, 1H, CHb-2 chrom.), 4.56–4.66 (m, 3H, CH₂-2 tasd, CH-4 chrom.), 6.75–7.00 (m, 5H, CH-2, CH-4, CH-6 arom. tasd; CH-6, CH-8 chrom.), 7.25 (m, 3H, CH-3, CH-5 arom. tasd; CH-7 chrom.), 7.55 ppm (d, $J = 7.5$ Hz, 1H, CH-5 chrom.).

HRMS-ESI m/z [M + H]⁺ calc. for C₂₂H₂₆N₃O₂: 364.2019; found: 364.2016; anal. calcd for C₂₄H₂₇N₃O₆: C, 63.56; H, 6.00; N, 9.27; found C, 63.31; H, 5.88; N, 9.03.

Biology

General. N/OFQ used in this study was prepared and purified as previously described.³⁵ All cell culture media and supplements were purchased from Invitrogen (Paisley, UK), SB-612111 was from Tocris Bioscience (Bristol, UK) and other reagents were purchased from Sigma Chemical Co. (Poole, UK) or from E. Merck (Darmstadt, Germany) and were of the highest purity available. N/OFQ was solubilized in bidistilled water at a final concentration of 1 mM. All the tested compounds were solubilized in dimethyl sulfoxide at a final concentration of 10 mM. Stock solutions of ligands were stored at –20 °C. The successive dilutions were made in HBSS–HEPES buffer (20 mM, containing 0.005% BSA fraction V).

Calcium mobilization assay. Chinese Hamster Ovary (CHO) cells, stably co-expressing human recombinant NOP receptors and the C-terminally modified Gα_{q15} protein, were generated as described by Camarda *et al.* (2009).²³

The cells were cultured in culture medium consisting of Dulbecco's MEM/HAMS F12 (50/50) supplemented with 10% foetal calf serum, penicillin (100 IU ml^{–1}), streptomycin (100 mg ml^{–1}), geneticin (G418, 200 µg ml^{–1}) and hygromycin B (100 µg ml^{–1}). Cell cultures were kept at 37 °C in 5% CO₂/

humidified air. When confluence was reached (3–4 days), cells were sub-cultured as required using trypsin/EDTA and used for experimentation. CHO_{NOP} stably expressing the Gα_{q15} protein was seeded at a density of 50 000 cells per well into 96-well black, clear-bottom plates. After 24 hours incubation, the cells were loaded with a medium supplemented with 2.5 mM probenecid, 3 µM of the calcium sensitive fluorescent dye Fluo-4 AM and with 0.01% pluronic acid, for 30 min at 37 °C. Afterwards the loading solution was aspirated and 100 µl per well of assay buffer, Hank's Balanced Salt Solution (HBSS) supplemented with 20 mM HEPES, 2.5 mM probenecid and 500 µM Brilliant Black, was added. After placing both plates (cell culture and compound plate) into the FlexStation II, fluorescence changes were measured.

Data analysis and terminology. All data are expressed as mean ± standard error of the mean (sem) of at least 3 experiments performed in duplicate. For potency values 95% confidence limits were indicated. Calcium mobilization data are expressed as fluorescence intensity units (FIU) in percent over the baseline. Agonist potencies are given as pEC₅₀ corresponding to the negative logarithm of the concentration of the agonist that produces 50% of the maximal effect. Concentration response curves to agonists were fitted by using the following equation:

$$\text{Effect} = \text{baseline} + \frac{E_{\text{max}} - \text{baseline}}{1 + 10^{(\log \text{EC}_{50} - X) \cdot n}}$$

where X is the agonist concentration and n is the Hill coefficient.

Agonist efficacy is expressed as intrinsic activity (α) using the maximal effect elicited by N/OFQ as an internal standard ($\alpha = 1.00$).

Antagonist potencies are given as pK_B values. These were derived from inhibition response curves and calculated, assuming a competitive type of antagonism, using the following equation:

$$\text{pK}_B = -\log \frac{\text{IC}_{50}}{\left(2 + \left(\frac{[A]}{\text{EC}_{50}}\right)^n\right)^{1/n}} - 1$$

where IC₅₀ is the concentration of the antagonist that produces 50% inhibition of the agonist response, $[A]$ is the concentration of the agonist, EC₅₀ is the concentration of the agonist that produces 50% of the maximal response and n is the Hill coefficient of the concentration response curve to the agonist.

Conclusions

In summary, we have developed several small molecule ligands for the NOP receptor, among them compound **4** demonstrated a good activity as a NOP receptor agonist. Then an enantioseparative method has been developed to obtain single enantiomers of **4**. Further biological studies have shown (*R*)-**4** as the eutomer, indicating a clear stereospecific interaction. Docking studies were performed on the NOP receptor crystal structure in order to understand the binding mode of the two stereoisomers

of 4. These results would help guide the further development of *N*-substituted spiropiperidine-based NOP agonists.

Acknowledgements

We thank Dr Samuele Ciattini (Centro di Cristallografia Strutturale, Università degli Studi di Firenze) for X-ray data collection.

Notes and references

- 1 J. C. Meunier, C. Mollereau, L. Toll, C. Suaudeau, C. Moisand, P. Alvinerie, J. L. Butour, J. C. Guillemot, P. Ferrara, B. Monsarrat, H. Mazarguil, G. Vassart, M. Parmentier and J. Costentin, *Nature*, 1995, **377**, 532–535.
- 2 R. K. Reinscheid, H. P. Nothacker, A. Bourson, A. Ardati, R. A. Henningsen, J. R. Bunzow, D. K. Grandy, H. Langen, F. J. Monsma and O. Civelli, *Science*, 1995, **270**, 792–794.
- 3 C. Mollereau, M. Parmentier, P. Mailleux, J. Butour, C. Moisand, P. Chalon, D. Caput, G. Vassart and J. C. Meunier, *FEBS Lett.*, 1994, **341**, 33–38.
- 4 K. Fukada, S. Kato, K. Mori, M. Nishi, H. Takeshima, N. Iwabe, T. Miyata, T. Houtani and T. Sugomoto, *FEBS Lett.*, 1994, **343**, 42–46.
- 5 Y. Chen, Y. Fan, J. Liu, A. Mestek, M. Tian, C. A. Kozak and L. Yu, *FEBS Lett.*, 1994, **347**, 279–283.
- 6 J. B. Wang, P. S. Johnson, Y. Imai, A. M. Persico, B. A. Ozenberger, C. M. Eppler and G. R. Uhl, *FEBS Lett.*, 1994, **348**, 75–79.
- 7 S. R. Singh, N. Sullo, B. D'Agostino, C. E. Brightling and D. G. Lambert, *Peptides*, 2013, **39**, 36–46.
- 8 E. C. Gavioli and G. Calò, *Pharmacol. Ther.*, 2013, **140**, 10–25.
- 9 N. T. Zaveri, *Curr. Top. Med. Chem.*, 2011, **11**, 1151–1156.
- 10 K. Tekes, S. Tariq, E. Adeghate, R. Laufer, F. Hashemi, A. Siddiq and H. Kalasz, *Mini-Rev. Med. Chem.*, 2013, **13**, 1389–1397.
- 11 G. Calò, R. Guerrini, A. Rizzi, S. Salvadori and D. Regoli, *Br. J. Pharmacol.*, 2000, **129**, 1261–1283.
- 12 D. G. Lambert, *Nat. Rev. Drug Discovery*, 2008, **7**, 694–710.
- 13 N. Zaveri, W. E. Polgar, C. M. Olsen, A. B. Kelson, P. Grundt, J. W. Lewis and L. Toll, *Eur. J. Pharmacol.*, 2001, **428**, 29–36.
- 14 N. Zaveri, *Life Sci.*, 2003, **73**, 663–678.
- 15 T. M. Largent-Milnes and T. W. Vanderah, *Expert Opin. Ther. Pat.*, 2010, **20**, 291–305.
- 16 C. Thomsen and R. Hohlweg, *Br. J. Pharmacol.*, 2000, **131**, 903–908.
- 17 N. Zaveri, F. Jiang, C. Olsen, W. Polgar and L. Toll, *AAPS J.*, 2005, **7**, E345–E352.
- 18 A. P. Lin and M. C. Ko, *ACS Chem. Neurosci.*, 2013, **4**, 214–224.
- 19 F. Jenck, F. J. Monsma, G. Galley, G. Adam, A. M. Cesura, S. Rover, J. Wichmann, *Ca. Pat.*, 2 226 058, 1998.
- 20 S. Oh, H. J. Nam, J. Park, S. H. Beak and S. B. Park, *ChemMedChem*, 2010, **5**, 529–533.
- 21 A. Yamashita, E. B. Norton, C. Hanna, J. Shim, E. J. Salaski, D. Zhou and T. S. Mansour, *Synth. Commun.*, 2005, **36**, 465–466.
- 22 B. Hua, F. Zewang, W. Jianhang, S. Lijie, *Cn. Pat.*, 101 497 612, 2009.
- 23 V. Camarda, C. Fischetti, N. Anzellotti, P. Molinari, C. Ambrosio, E. Kostenis, D. Regoli, C. Trapella, R. Guerrini, S. Salvadori and G. Calò, *Naunyn-Schmiedeberg's Arch. Pharmacol.*, 2009, **379**, 599–607.
- 24 C. Fischetti, V. Camarda, A. Rizzi, M. Pelà, C. Trapella, R. Guerrini, J. McDonald, D. G. Lambert, S. Salvadori, D. Regoli and G. Calò, *Eur. J. Pharmacol.*, 2009, **614**, 50–57.
- 25 C. Trapella, C. Fischetti, M. Pela, I. Lazzari, R. Guerrini, G. Calò, A. Rizzi, V. Camarda, D. G. Lambert, J. McDonald, D. Regoli and S. Salvadori, *Bioorg. Med. Chem.*, 2009, **17**, 5080–5095.
- 26 S. Molinari, V. Camarda, A. Rizzi, G. Marzola, S. Salvadori, E. Marzola, P. Molinari, J. McDonald, M. C. Ko, D. G. Lambert, G. Calò and R. Guerrini, *Br. J. Pharmacol.*, 2013, **168**, 151–162.
- 27 P. F. Zaratin, G. Petrone, M. Sbacchi, M. Garnier, C. Fossati, P. Petrillo, S. Ronzoni, G. A. Giardina and M. A. Scheideler, *J. Pharmacol. Exp. Ther.*, 2004, **308**, 454–461.
- 28 M. Marti, F. Mela, M. Budri, M. Volta, D. Malfacini, S. Molinari, N. T. Zaveri, S. Ronzoni, P. Petrillo, G. Calò and M. Morari, *J. Pharmacol.*, 2013, **168**, 863–879.
- 29 S. Rover, G. Adam, A. M. Cesura, G. Galley, F. Jenck, F. J. Monsma, J. Wichmann and F. M. Dautzenber, *J. Med. Chem.*, 2000, **43**, 1329–1338.
- 30 A. Beecham, *J. Am. Chem. Soc.*, 1957, **79**, 3257–3261.
- 31 A. A. Thompson, W. Liu, E. Chun, V. Katritch, H. Wu, E. Vard, X. P. Huang, C. Trapella, R. Guerrini, G. Calò, B. L. Roth, V. Cherezov and R. C. Stevens, *Nature*, 2012, **485**, 395–399.
- 32 V. Katritch and R. Abagyan, *Trends Pharmacol. Sci.*, 2011, **32**, 637–643.
- 33 H. O. Onaran and T. Costa, *Nat. Chem. Biol.*, 2012, **8**, 674–677.
- 34 L. Mouledous, C. M. Topham, C. Moisand, C. Mollereau and J. C. Meunier, *Mol. Pharmacol.*, 2000, **57**, 495–502.
- 35 R. Guerrini, G. Calò, A. Rizzi, C. Bianchi, L. H. Lazarus, S. Salvadori, P. A. Temussi and D. Regoli, *J. Med. Chem.*, 1997, **40**, 1789–1793.